ACS APPLIED MATERIALS & INTERFACES

Research Article

www.acsami.org

Simple Method to Enhance Positive Bias Stress Stability of In−Ga−Zn−O Thin-Film Transistors Using a Vertically Graded Oxygen-Vacancy Active Layer

Ji Hoon Park,‡ Yeong-gyu Kim,‡ Seokhyun Yoon, Seonghwan Hong, and Hyun Jae Kim*

School of Electrical and Electronic Engineering, Yonsei University, 50 Yonsei-ro, Seodaemun-gu, Seoul 120-749, Republic of Korea

ABSTRACT: We proposed a simple method to deposit a vertically graded oxygen-vacancy active layer (VGA) to enhance the positive bias stress (PBS) stability of amorphous indium gallium zinc oxide (a-IGZO) thin-film transistors (TFTs). We deposited a-IGZO films by sputtering (target composition; In_2O_3:Ga_2O_3:ZnO = 1:1:1 mol %), and the oxygen partial pressure was varied during deposition so that the front channel of the TFTs was fabricated with low oxygen partial pressure and the back channel with high oxygen partial pressure. Using this method, we were able to control the oxygen vacancy concentration of the active layer so that it varied with depth. As a result, the turn-on voltage shift following a 10 000 s PBS of optimized VGA TFT was drastically improved from 12.0 to 5.6 V compared with a conventional a-IGZO TFT, without a significant decrease in the field effect mobility. These results came from the self-passivation effect and decrease in oxygen-vacancy-related trap sites of the VGA TFTs.

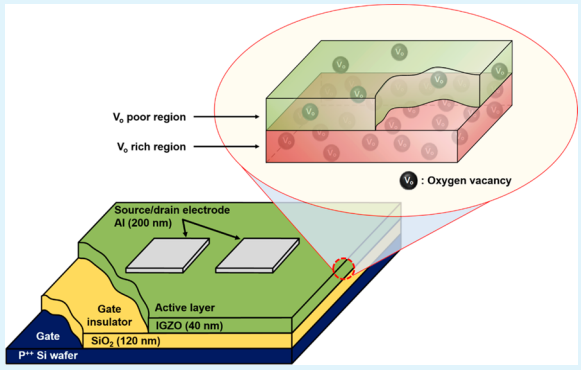

KEYWORDS: *oxide semiconductor, thin-film transistors, bias stability, In−Ga−Zn−O, oxygen vacancy*

1. INTRODUCTION

Amorphous oxide semiconductors (AOSs) have attracted considerable research attention in recent years as an active layer material for use in thin-film transistors (TFTs) because of their superior electrical characteristics compared with conventional amorphous Si.[1−3] AOSs exhibit many advantages in terms of electron mobility, transparency in visible wavelengths, and uniformity for large area fabrication.[4−6] Moreover, the low-temperature deposition process of AOSs makes it possible to deposit the active layer materials on flexible substrates.[7−9] In spite of these advantages, instabilities of AOSs in response to various stress conditions such as illumination, bias, current, and temperature remain an issue.[10−12] These instabilities are a critical problem that must be addressed to utilize AOSs in TFT applications. A number of reports have proposed methods to enhance the stability of AOS TFTs, including high-pressure annealing,[13] gate insulator modification,[14] and additional plasma treatment on the active layer.[15,16] However, these methods require additional process steps, leading to increased complexity of the process and manufacturing costs.

It has been reported that positive bias stress (PBS) stability can be improved by controlling oxygen vacancy (V_O) concentration in the active layer.[17,18] It is well-known that the V_O in oxide semiconductors acts as a carrier supplier, so it contributes to current flow.[19,20] It has also been reported that the V_O in the active layer leads to instabilities of electrical properties under PBS because it can act as electron trap sites.[21,22] Thus, a high concentration of V_O in the active layer may lead to favorable electrical performance but is also a major cause of poor PBS stability. It follows that control over the concentration of V_O in the active layer is important in AOS TFTs.

In this study, we developed a simple method to fabricate a vertically graded V_O active layer (VGA) by varying the oxygen partial pressure during active layer deposition to control the V_O concentration according to the depth. This simple method leads to PBS stability improvement of TFTs without additional complex processes.

2. EXPERIMENTAL SECTION

2.1. Fabrication of TFTs. We fabricated the a-IGZO TFTs with inverted staggered structure using a heavily doped p-type Si wafer with thermally oxidized SiO_2 of 1200 Å as a substrate. The 40 nm thick a-IGZO active layer was deposited by radio frequency (RF) magnetron sputtering on the cleaned substrate by using a 3 in. IGZO target (In_2O_3:Ga_2O_3:ZnO = 1:1:1 mol %). The RF power was 150 W; the working pressure was 5 mTorr; the total deposition time was 300 s; and the process was carried out at room temperature. We set the oxygen partial pressure ($[O_2]/[Ar + O_2]$) to 0% to fabricate the V_O-rich film and 5% to deposit the V_O-poor film. To fabricate the VGA, the oxygen partial pressure was increased from 0% to 5% during fabrication, whereas the oxygen partial pressure was fixed at either 0% or 5% to fabricate the conventional TFTs used for reference. Active layers were fabricated with different time for the 0% oxygen partial pressure and 5% oxygen partial pressure, i.e., time ratios of 0% and 5% and oxygen partial pressures of 100:0, 75:25, 50:50, 25:75, and 0:100;

Received: September 15, 2014
Accepted: November 17, 2014
Published: November 17, 2014

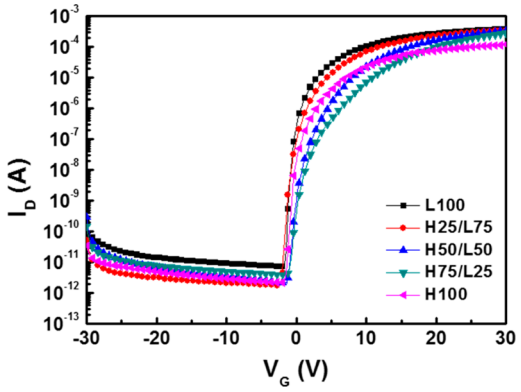

Figure 1. Transfer characteristics of conventional and VGA TFTs with various thickness ratios of the V_O-poor to V_O-rich regions.

these samples are henceforth termed L100, H25/L75, H50/L50, H75/L25, and H100, respectively. These deposition time ratios were directly related to the thickness ratio of the V_O-rich region to V_O-poor region. Following deposition of the active layer, the samples were annealed at 300 °C for 1 h in ambient air. Aluminum source/drain electrodes with a thickness of 200 nm were deposited using thermal evaporation via a shadow mask. The width and length of the channel were 1000 and 150 μm, respectively.

2.2. Electrical and Chemical Characteristic Measurement. The current−voltage (I−V) characteristics of the fabricated TFTs were measured using an HP4156C semiconductor parameter analyzer in the dark and at room temperature. The electrical parameters of the TFTs were analyzed from their transfer characteristics with a drain voltage (V_D) of 10.1 V in this work. The field effect mobility (μ_{FE}) was extracted from the transfer characteristics using the following relation

$$\mu_{FE} = \left(\frac{2}{C_{ox}}\right)\left(\frac{L}{W}\right)(G_{max})^2$$

where C_{ox} is the gate insulator capacitance per unit area; L/W is the ratio of length to width; and G_{max} is the derivative maximum of the square root of the drain current with respect to the square root of the gate voltage, i.e.

$$G = \frac{\partial\sqrt{I_D}}{\partial\sqrt{V_G}}$$

Additionally, we performed depth profile X-ray photoelectron spectroscopy (XPS) to investigate the chemical composition of the films.

3. RESULTS AND DISCUSSION

Figure 1 shows the transfer characteristics of the conventional and VGA a-IGZO TFTs. As the thickness of the high oxygen partial pressure layer increased, both the on-current and μ_{FE} decreased. The L100 TFT deposited by conventional methods with low oxygen partial pressure exhibited the highest μ_{FE} of 10.77 $cm^2/(V\ s)$, whereas the H100 TFT exhibited the lowest μ_{FE} of 3.06 $cm^2/(V\ s)$. The VGA TFTs with the H25/L75 and H50/L50 showed the μ_{FE} of 9.27 and 8.04 $cm^2/(V\ s)$, respectively, and these values were slightly decreased in μ_{FE} compared with the L100 TFT. However, the μ_{FE} of the H75/L25 TFT was 6.52 $cm^2/(V\ s)$, and this value was degraded about 40% compared with the L100 TFT. Because we are interested in improving the PBS stability without degrading the electrical characteristics, we did not investigate the H75/L25 TFT further. Consequently, the PBS tests were carried out for the H25/L75 and H50/L50 among the VGA TFTs and for L100 and H100 as the reference, respectively.

The PBS tests were performed with V_{GS} = 20 V and V_{DS} = 10.1 V, applied for 1000 s. The variation of turn-on voltage (V_{on}) shift was investigated to compare the PBS stability of the TFTs. Figure 2a−c shows the evolution of the transfer characteristics of the L100, H25/L75, and H50/L50 TFTs.

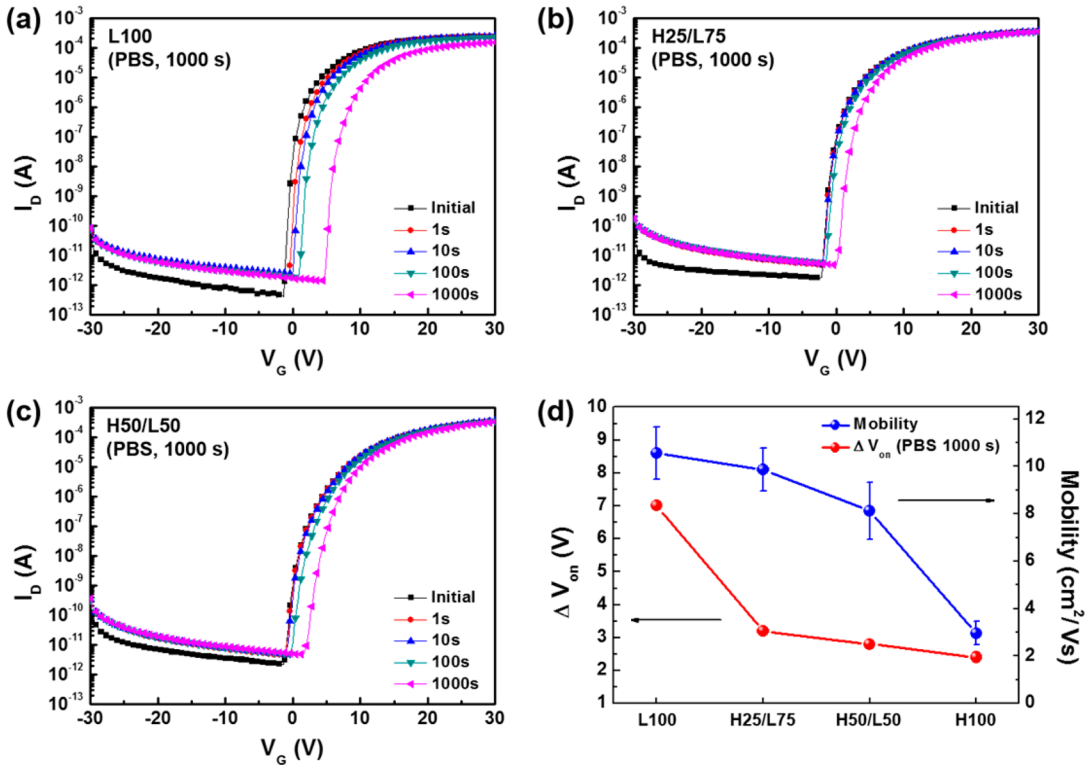

Figure 2. PBS test results of a-IGZO TFTs with (a) L100, (b) H25/L75, and (c) H50/L50. (d) Variation in μ_{FE} and V_{on} shift after the 1000 s PBS tests.

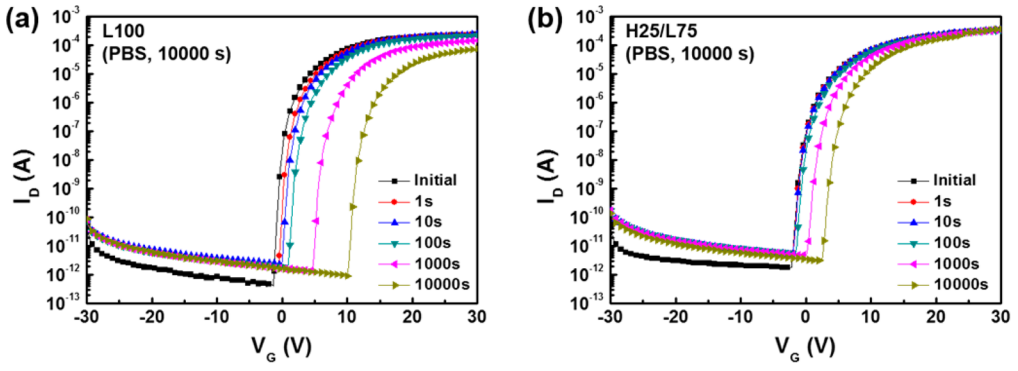

Figure 3. Transfer characteristic of a-IGZO TFT with (a) L100 and (b) H25/L75 as a function of the applied PBS time.

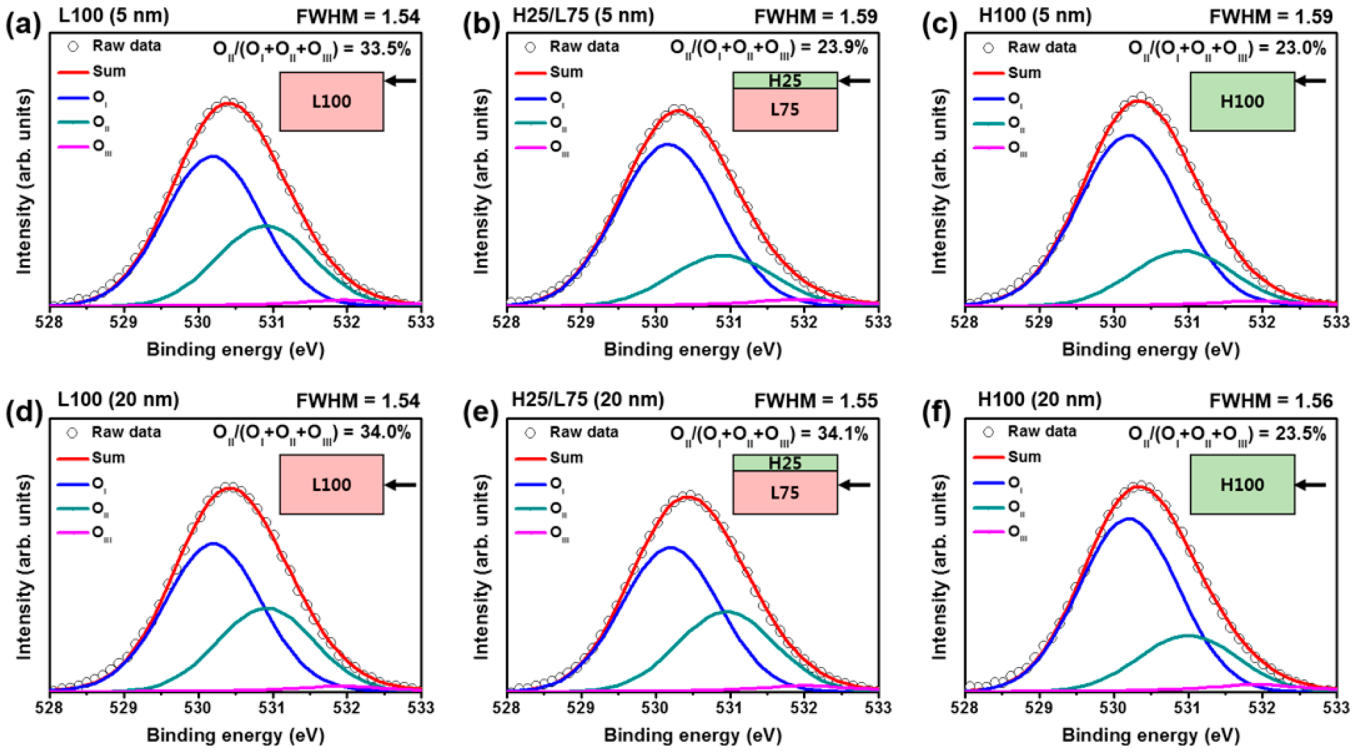

Figure 4. XPS results for the O 1s peak for different a-IGZO films at different depths: (a) L100, (b) H25/L75, and (c) H100 at 5 nm from the surface and (d) L100, (e) H25/L75, and (f) H100 at 20 nm from the surface.

The V_{on} shift of L100 TFT after 1000 s was 7.0 V, and it was the worst PBS stability among the all TFTs. The H25/L75 and H50/L50 TFTs showed V_{on} shifts of 3.2 and 2.8 V, respectively. Figure 2d shows the variation in μ_{FE} and V_{on} shift after the 1000 s PBS for each TFT. The PBS stability of VGA TFTs was drastically improved compared with the L100 TFT. Furthermore, as the thickness of the high oxygen partial pressure layer increased, the PBS stability of the a-IGZO TFT also improved, while the μ_{FE} decreased. The H25/L75 TFT showed superior PBS stability compared with L100 TFT without a significant decrease in μ_{FE}. The H50/L50 TFT also showed improved PBS stability; however, the decrease in μ_{FE} was larger, and the PBS stability was not significantly improved compared with that of H25/L75 TFT. Therefore, the optimal VGA condition was H25/L75.

We performed an additional 10 000 s PBS test on the L100 and H25/L75 TFTs, as shown in Figure 3. The V_{on} shift of H25/L75 TFT after a 10 000 s PBS was 5.6 V, whereas that of the L100 TFT was 12.0 V. These results show that the PBS stability of the H25/L75 TFT was improved by a factor of more than 2 in terms of V_{on} shift without a significant change in μ_{FE} compared with the L100 TFT.

We performed depth profile XPS analyses to examine the chemical and structural changes related to the oxygen according to the depth. The binding energy was referenced to the C 1s peak centered at 284.8 eV for calibration, and the O 1s spectra were deconvoluted into three different peaks centered at 530.1 ± 0.1, 531.0 ± 0.1, and 532.0 ± 0.1 eV. The first peak with a low binding energy region (O_I) corresponds to lattice oxygen related to In, Ga, and Zn metal−oxide bonds (M−O). The medium binding energy region (O_{II}) corresponds to the metal oxide lattice with V_O, and the high binding energy region (O_{III}) represents metal hydroxide species (M−OH).[23,24] Figure 4a−c shows the O 1s spectra of the three a-IGZO samples at 5 nm from the surface, and Figure 4d−f shows the O 1s spectra at 20 nm from the surface. As shown in Figure 4a and c, the

dx.doi.org/10.1021/am5063212 | ACS Appl. Mater. Interfaces 2014, 6, 21363−21368

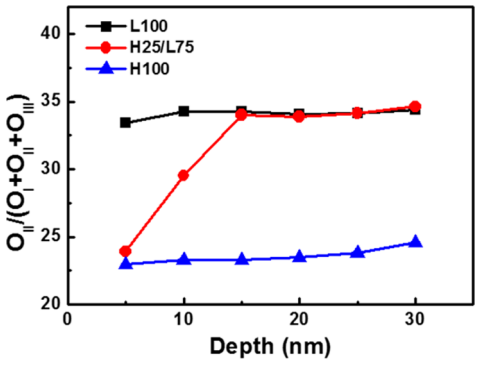

Figure 5. Comparison of the samples with the area ratio of the middle binding energy as a function of depth.

relative area of O_{II} (O_{II}') of the L100 sample was larger than that in the H100 sample. In other words, the films deposited with a lower oxygen partial pressure exhibited V_O-rich regions, i.e., a high V_O concentration.[25,26] The XPS data of the samples fabricated with conventional growth (i.e., L100 and H100) did not change with depth, as shown in Figure 4d and f. Therefore, L100 and H100 samples exhibited a uniform distribution of oxygen-related bonds, such as M−O, V_O, and M−OH regardless of the depth. However, for the H25/L75 sample, the XPS result at 5 nm from the surface exhibited a V_O-poor region, whereas at 20 nm from the surface it exhibited a V_O-rich region as shown in Figure 4b and e.

Figure 5 shows O_{II}' data as a function of the depth from the surface. As mentioned before, the H25/L75 sample showed variation in the V_O concentration with depth, whereas the L100 and H100 samples exhibited constant V_O concentrations. Because V_O in oxide semiconductors acts as a carrier supplier,[27−29] an increase in the V_O concentration leads to an increase in the carrier concentration of the film. High carrier concentration of the film can bring the high mobility because of a percolation conduction mechanism.[30,31] In this context, the high mobility of the L100 and H25/L75 TFTs may result from the high V_O concentration in the front channel because the effective channel region of the TFTs is formed near the gate insulator in the active layer.[32,33] The improvement in PBS stability of the H25/L75 TFT may be explained by considering the reduced V_O concentration of the back channel area compared with that of the L100 TFT. One of the major causes of PBS instability is the reaction between the back channel and the ambient air.[34] It has been shown that low V_O concentration in the back channel region inhibits reactions between the back channel and the ambient air.[35−37] In other words, a back channel region with low V_O concentration can act as a self-passivation layer. For this reason, the V_O-poor back channel of VGA TFTs may act as a self-passivation layer, so it decreases the interaction between the exposed back surface and the ambient atmosphere. Therefore, the VGA TFTs showed improved PBS stability compared to the L100 TFT.

Additionally, V_O in the active layer can act as an electron trap site, leading to PBS instabilities.[38,39] Therefore, the PBS stability improvement of the VGA TFTs with thicker V_O-poor layers may be expected because of an overall decrease in the concentration of V_O-related trap sites in the active layer. However, in this study, the interaction between the back surface and the ambient air is expected to be the dominant cause of PBS instability. It is consistent with the drastic improvement in the PBS stability of the H25/L75 TFT compared with the L100 TFT and with the insignificant improvement in the PBS stability of the H50/L50 and H100 TFT compared with the H25/L75 TFT. Figure 6 shows a schematic diagram of the VGA TFT structure. The active layer region near the gate insulator had high V_O concentration, whereas the active layer region far from the gate insulator had low V_O concentration. The improved PBS stability of the VGA TFT is attributed to self-passivation effects of the back surface region and a decrease in V_O-related electron trap sites.

4. CONCLUSION

We have described a simple method to improve the PBS stability of a-IGZO TFTs by controlling the oxygen partial pressure during deposition of the active layer. We deposited a V_O-rich film at the front channel using low oxygen partial

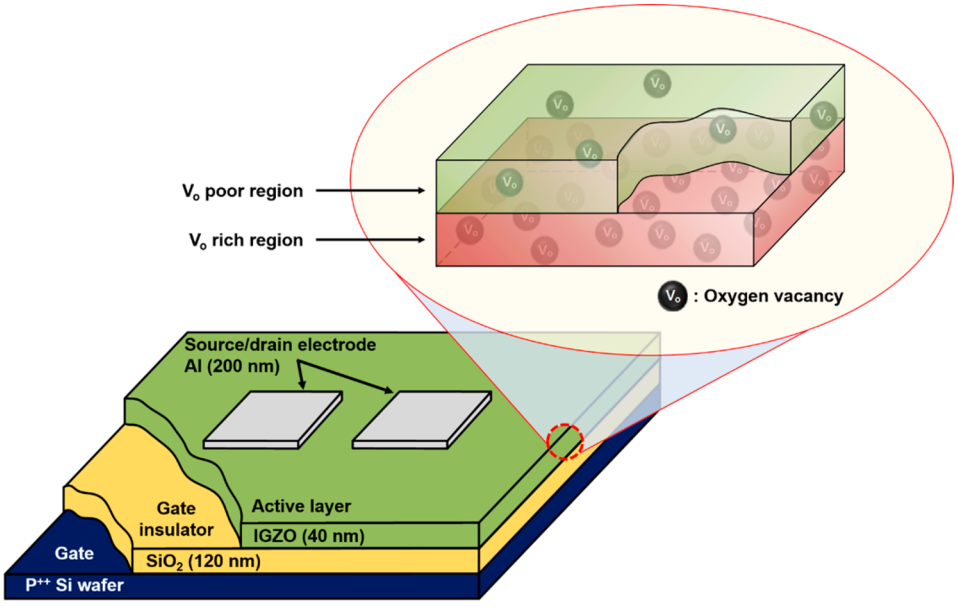

Figure 6. Schematic diagram of the VGA TFT structure.

pressure and V_O-poor film at the back channel using high oxygen partial pressure. Such vertical control over the V_O concentration in the active layer enabled us to fabricate a-IGZO TFTs with μ_{FE} of 9.21 $cm^2/(V\ s)$ and V_{on} shift of 5.6 V following a 10 000 s PBS test when the thickness ratio of the V_O-poor region to V_O-rich region was 25:75. These results showed that the PBS stability was improved by a factor of more than 2 in terms of V_{on} shift with a decrease in μ_{FE} of only 10% compared with the a-IGZO TFT fabricated with a conventional process. The improvement in the PBS stability was attributed to the self-passivation effect at the back surface and a decrease in the V_O-related trap site of the VGA TFTs. As a result, we confirmed that the VGA method by controlling oxygen partial pressure during film deposition is a simple and effective process to improve the PBS stability without an increase in manufacturing cost and process complexity.

AUTHOR INFORMATION

Corresponding Author

*E-mail: hjk3@yonsei.ac.kr.

Author Contributions

‡These authors contributed equally.

Notes

The authors declare no competing financial interest.

ACKNOWLEDGMENTS

This work was supported by Samsung Display and the National Research Foundation of Korea (NRF) grant funded by the Korea government (MSIP) (No. 2011-0028819).

REFERENCES

(1) Nomura, K.; Ohta, H.; Takagi, A.; Kamiya, T.; Hirano, M.; Hosono, H. Room-Temperature Fabrication of Transparent Flexible Thin-Film Transistors Using Amorphous Oxide Semiconductors. *Nature* **2004**, *432*, 488−492.

(2) Kumomi, H.; Nomura, K.; Kamiya, T.; Hosono, H. Amorphous Oxide Channel TFTs. *Thin Solid Films* **2008**, *516*, 1516−1522.

(3) Martins, R.; Raniero, L.; Pereira, L.; Costa, D.; Aguas, H.; Pereira, S.; Silva, L.; Gonçalves, A.; Ferreira, I.; Fortunato, E. Nanostructured Silicon and Its Application to Solar Cells, Position Sensors and Thin Film Transistors. *Philos. Mag.* **2009**, *89*, 2699−2721.

(4) Fortunato, E.; Barquinha, P.; Martins, R. Oxide Semiconductor Thin-Film Transistors: A Review of Recent Advances. *Adv. Mater.* **2012**, *24*, 2945−2986.

(5) Heo, S. J.; Choi, J.; Yoon, D. H.; Jung, T. S.; Kim, H. J. Recent Advances in Low-Temperature Solution-Processed Oxide Backplanes. *J. Inf. Disp.* **2013**, *14*, 79−87.

(6) Kim, S. J.; Yoon, S.; Kim, H. J. Review of Solution-Processed Oxide Thin-Film Transistors. *Jpn. J. Appl. Phys.* **2014**, *53*, 02BA02.

(7) Yabuta, H.; Sano, M.; Abe, K.; Aiba, T.; Den, T.; Kumomi, H.; Nomura, K.; Kamiya, T.; Hosono, H. High-Mobility Thin-Film Transistor with Amorphous $InGaZnO_4$ Channel Fabricated by Room Temperature RF-Magnetron Sputtering. *Appl. Phys. Lett.* **2006**, *89*, 112123.

(8) Lim, W.; Jang, J. H.; Kim, S.-H.; Norton, D.; Craciun, V.; Pearton, S.; Ren, F.; Shen, H. High Performance Indium Gallium Zinc Oxide Thin Film Transistors Fabricated on Polyethylene Terephthalate Substrates. *Appl. Phys. Lett.* **2008**, *93*, 082102.

(9) Kim, Y.-H.; Heo, J.-S.; Kim, T.-H.; Park, S.; Yoon, M.-H.; Kim, J.; Oh, M. S.; Yi, G.-R.; Noh, Y.-Y.; Park, S. K. Flexible Metal-Oxide Devices Made by Room-Temperature Photochemical Activation of Sol-Gel Films. *Nature* **2012**, *489*, 128−132.

(10) Kang, D.; Lim, H.; Kim, C.; Song, I.; Park, J.; Park, Y.; Chung, J. Amorphous Gallium Indium Zinc Oxide Thin Film Transistors: Sensitive to Oxygen Molecules. *Appl. Phys. Lett.* **2007**, *90*, 192101.

(11) Cross, R.; De Souza, M. Investigating the Stability of Zinc Oxide Thin Film Transistors. *Appl. Phys. Lett.* **2006**, *89*, 263513.

(12) Ryu, B.; Noh, H.-K.; Choi, E.; Chang, K. O-Vacancy as the Origin of Negative Bias Illumination Stress Instability in Amorphous In−Ga−Zn−O Thin Film Transistors. *Appl. Phys. Lett.* **2010**, *97*, 022108.

(13) Rim, Y. S.; Jeong, W. H.; Kim, D. L.; Lim, H. S.; Kim, K. M.; Kim, H. J. Simultaneous Modification of Pyrolysis and Densification for Low-Temperature Solution-Processed Flexible Oxide Thin-Film Transistors. *J. Mater. Chem.* **2012**, *22*, 12491−12497.

(14) Oh, M. S.; Lee, K.; Song, J.; Lee, B. H.; Sung, M. M.; Hwang, D.; Im, S. Improving the Gate Stability of ZnO Thin-Film Transistors with Aluminum Oxide Dielectric Layers. *J. Electrochem. Soc.* **2008**, *155*, H1009−H1014.

(15) Tsai, C.-T.; Chang, T.-C.; Chen, S.-C.; Lo, I.; Tsao, S.-W.; Hung, M.-C.; Chang, J.-J.; Wu, C.-Y.; Huang, C.-Y. Influence of Positive Bias Stress on N_2O Plasma Improved InGaZnO Thin Film Transistor. *Appl. Phys. Lett.* **2010**, *96*, 242105.

(16) Yang, S.; Hwan Ji, K.; Ki Kim, U.; Seong Hwang, C.; Ko Park, S.-H.; Hwang, C.-S.; Jang, J.; Jeong, J. K. Suppression in the Negative Bias Illumination Instability of Zn-Sn-O Transistor Using Oxygen Plasma Treatment. *Appl. Phys. Lett.* **2011**, *99*, 102103.

(17) Rim, Y. S.; Kim, D. L.; Jeong, W. H.; Kim, H. J. Improved Bias Stability of Solution-Processed ZnSnO Thin-Film Transistors by Zr Addition. *Electrochem. Solid-State Lett.* **2011**, *15*, H37−H40.

(18) Jun, T.; Song, K.; Jung, Y.; Jeong, S.; Moon, J. Bias Stress Stable Aqueous Solution Derived Y-Doped ZnO Thin Film Transistors. *J. Mater. Chem.* **2011**, *21*, 13524−13529.

(19) Jeong, W. H.; Kim, G. H.; Shin, H. S.; Du Ahn, B.; Kim, H. J.; Ryu, M.-K.; Park, K.-B.; Seon, J.-B.; Lee, S. Y. Investigating Addition Effect of Hafnium in InZnO Thin Film Transistors Using a Solution Process. *Appl. Phys. Lett.* **2010**, *96*, 093503.

(20) Yao, J.; Xu, N.; Deng, S.; Chen, J.; She, J.; Shieh, H.; Liu, P.-T.; Huang, Y.-P. Electrical and Photosensitive Characteristics of a-IGZO TFTs Related to Oxygen Vacancy. *IEEE Trans. Electron Devices* **2011**, *58*, 1121−1126.

(21) Jeong, Y.; Bae, C.; Kim, D.; Song, K.; Woo, K.; Shin, H.; Cao, G.; Moon, J. Bias-Stress-Stable Solution-Processed Oxide Thin Film Transistors. *ACS Appl. Mater. Interfaces* **2010**, *2*, 611−615.

(22) Chong, E.; Jo, K. C.; Lee, S. Y. High Stability of Amorphous Hafnium-Indium-Zinc-Oxide Thin Film Transistor. *Appl. Phys. Lett.* **2010**, *96*, 152102.

(23) Tak, Y. J.; Yoon, D. H.; Yoon, S.; Choi, U. H.; Sabri, M. M.; Ahn, B. D.; Kim, H. J. Enhanced Electrical Characteristics and Stability Via Simultaneous Ultraviolet and Thermal Treatment of Passivated Amorphous In−Ga−Zn−O Thin-Film Transistors. *ACS Appl. Mater. Interfaces* **2014**, *6*, 6399−6405.

(24) Kang, J. H.; Cho, E. N.; Kim, C. E.; Lee, M.-J.; Lee, S. J.; Myoung, J.-M.; Yun, I. Mobility Enhancement in Amorphous InGaZnO Thin-Film Transistors by Ar Plasma Treatment. *Appl. Phys. Lett.* **2013**, *102*, 222103.

(25) Moon, Y.-K.; Moon, D.-Y.; Lee, S.; Lee, S.-H.; Park, J.-W.; Jeong, C.-O. Effects of Oxygen Contents in the Active Channel Layer on Electrical Characteristics of ZnO-Based Thin Film Transistors. *J. Vac. Sci. Technol., B* **2008**, *26*, 1472−1476.

(26) Liang, C.-H.; Chau, J. L. H.; Yang, C.-C.; Shih, H.-H. Preparation of Amorphous Ga−Sn−Zn−O Semiconductor Thin Films by RF-Sputtering Method. *Mater. Sci. Eng., B* **2014**, *183*, 17−23.

(27) Vygranenko, Y.; Wang, K.; Nathan, A. Stable Indium Oxide Thin-Film Transistors with Fast Threshold Voltage Recovery. *Appl. Phys. Lett.* **2007**, *91*, 263508.

(28) Kim, G. H.; Jeong, W. H.; Du Ahn, B.; Shin, H. S.; Kim, H. J.; Kim, H. J.; Ryu, M.-K.; Park, K.-B.; Seon, J.-B.; Lee, S.-Y. Investigation of the Effects of Mg Incorporation into InZnO for High-Performance and High-Stability Solution-Processed Thin Film Transistors. *Appl. Phys. Lett.* **2010**, *96*, 163506.

(29) Lee, S.; Paine, D. C. Identification of the Native Defect Doping Mechanism in Amorphous Indium Zinc Oxide Thin Films Studied

Using Ultra High Pressure Oxidation. *Appl. Phys. Lett.* **2013**, *102*, 052101.
(30) Nomura, K.; Takagi, A.; Kamiya, T.; Ohta, H.; Hirano, M.; Hosono, H. Amorphous Oxide Semiconductors for High-Performance Flexible Thin-Film Transistors. *Jpn. J. Appl. Phys.* **2006**, *45*, 4303.
(31) Ahn, B. D.; Shin, H. S.; Kim, H. J.; Park, J.-S.; Jeong, J. K. Comparison of the Effects of Ar and H_2 Plasmas on the Performance of Homojunctioned Amorphous Indium Gallium Zinc Oxide Thin Film Transistors. *Appl. Phys. Lett.* **2008**, *93*, 203506.
(32) Kim, D. J.; Kim, D. L.; Rim, Y. S.; Kim, C. H.; Jeong, W. H.; Lim, H. S.; Kim, H. J. Improved Electrical Performance of an Oxide Thin-Film Transistor Having Multi-Stacked Active Layers Using a Solution Process. *ACS Appl. Mater. Interfaces* **2012**, *4*, 4001−4005.
(33) Fortunato, E.; Barquinha, P.; Pimentel, A.; Goncalves, A.; Marques, A.; Pereira, L.; Martins, R. Recent Advances in ZnO Transparent Thin Film Transistors. *Thin Solid Films* **2005**, *487*, 205−211.
(34) Jeong, J. K.; Yang, W. H.; Jeong, J. H.; Mo, Y.-G.; Kim, H. D. Origin of Threshold Voltage Instability in Indium-Gallium-Zinc Oxide Thin Film Transistors. *Appl. Phys. Lett.* **2008**, *93*, 123508.
(35) Kim, D. J.; Rim, Y. S.; Kim, H. J. Enhanced Electrical Properties of Thin-Film Transistor with Self-Passivated Multistacked Active Layers. *ACS Appl. Mater. Interfaces* **2013**, *5*, 4190−4194.
(36) Kim, C. H.; Rim, Y. S.; Kim, H. J. Chemical Stability and Electrical Performance of Dual-Active-Layered Zinc−Tin−Oxide/Indium−Gallium−Zinc−Oxide Thin-Film Transistors Using a Solution Process. *ACS Appl. Mater. Interfaces* **2013**, *5*, 6108−6112.
(37) Chong, E.; Lee, S. Y. Influence of a Highly Doped Buried Layer for HfInZnO Thin-Film Transistors. *Semicond. Sci. Technol.* **2012**, *27*, 012001.
(38) Jeong, Y.; Song, K.; Kim, D.; Koo, C. Y.; Moon, J. Bias Stress Stability of Solution-Processed Zinc Tin Oxide Thin-Film Transistors. *J. Electrochem. Soc.* **2009**, *156*, H808−H812.
(39) Jeong, Y.; Song, K.; Jun, T.; Jeong, S.; Moon, J. Effect of Gallium Content on Bias Stress Stability of Solution-Deposited Ga−Sn−Zn−O Semiconductor Transistors. *Thin Solid Films* **2011**, *519*, 6164−6168.